Polymer 203 (2020) 122786

Contents lists available at ScienceDirect

Polymer

journal homepage: http://www.elsevier.com/locate/polymer

Localizing and quantifying the intra-monomer contributions to the glass transition temperature using artificial neural networks

Luis A. Miccio [a,b,c,*], Gustavo A. Schwartz [a,b,**]

[a] Centro de Física de Materiales (CSIC-UPV/EHU) - Materials Physics Center (MPC), P. M. de Lardizábal 5, 20018, San Sebastián, Spain
[b] Donostia International Physics Center, P. M. de Lardizábal 4, 20018, San Sebastián, Spain
[c] Institute of Materials Science and Technology (INTEMA), National Research Council (CONICET), Colón 10850, 7600, Mar del Plata, Buenos Aires, Argentina

ARTICLE INFO

Keywords:
QSPR
Properties prediction
Polymers
Artificial neural networks
Smart design

ABSTRACT

We used fully connected artificial neural networks (ANN) to localize and quantify, based on the monomer structure of several polymers, the specific features responsible for their observed glass transition temperatures (T_g). The use of ANNs allows us not only to successfully predict the T_g of the polymers but, even more important, to understand what parts of the monomer are mainly contributing to it. For this task, we used the weights of a trained ANN as obtained after fitting the input data (monomer structure) to the corresponding T_g value. The study was performed for a set of more than 200 atactic acrylates for which typical T_g defining features were identified. Thus, the ANN is able to recognize the relevance of the backbone stiffness, the length of pending groups or the presence of methyl groups on the value of the glass transition temperature. This approach can be easily extended to many other interesting properties of polymers and it is worth noting that only the monomer chemical structure is needed as input. This method is potentially useful for identifying orthogonal ways of tuning polymer properties during the design and development of new materials and it is expected that it will contribute to a better understanding of the polymer's behavior.

1. Introduction

In the last decades, Quantitative Structure Property Relationship (QSPR) models have been successfully employed in the design and development of new materials with specific properties [1]. Their predictive power has been used for estimating the value of very different material properties like glass transition temperatures (T_g), boiling points, partition coefficients and toxicity, among many others [2–11]. The value of these approaches is even greater in the case of time consuming or expensive experiments, where every insight saves vast amounts of time and money to scientists and companies.

Among the many available tools for QSPR models, it is particularly interesting the case of artificial neural networks (ANNs). Several works [7,10,12,13] have been conducted by constructing a dataset with the values of selected material properties from either experimental results or literature search, and using ANNs for learning and predicting other properties from them. In this pursuit, different ANNs architectures and codifications have been proposed [7,13]. In a previous work [14] we have shown that ANNs can be trained using only a representation of the monomer chemical structure (as input) and a given property (T_g) as output. That approach provides an accuracy for the T_g predictions in the range of 94%. However, a common issue with all these methods is, bluntly speaking, their lack of transparency i.e.: the ANNs act as black boxes where properly codified information is fed into the network and a given output value or classification is obtained. With some exceptions, no information on which elements of the input data is responsible of the output results can be obtained.

For a given property, the ANN training process can be thought as a two-fold process: a) the mining of (related) critical information hidden in the multidimensional training data (features) and b) the correlation of these features to the real property value for constructing the prediction. It is therefore reasonable to think that these features, if accessible, might be employed for studying the physical mechanisms involved in the emergence of a given property.

In this work we propose a novel approach to find and show the relationship between the features extracted by the ANN from the chemical structure and the observed polymer property. In this way, we are able to localize and quantify the intra-monomer contributions to the

* Corresponding author. Centro de Física de Materiales (CSIC-UPV/EHU) - Materials Physics Center (MPC), P. M. de Lardizábal 5, 20018, San Sebastián, Spain.
** Corresponding author. Centro de Física de Materiales (CSIC-UPV/EHU) - Materials Physics Center (MPC), P. M. de Lardizábal 5, 20018, San Sebastián, Spain.
E-mail addresses: lamiccio@gmail.com (L.A. Miccio), gustavo.schwartz@csic.es (G.A. Schwartz).

https://doi.org/10.1016/j.polymer.2020.122786
Received 27 April 2020; Received in revised form 3 July 2020; Accepted 4 July 2020
Available online 16 July 2020
0032-3861/

glass transition temperature. In order to obtain a proof of concept, we used a dataset composed by more than 200 atactic acrylates. After training the ANN with this dataset, we can find, for new polymers (not included in the training dataset), not only the value of the glass transition temperature but also the contribution of each part of the monomer to the corresponding T_g.

2. Method

In this section we explain the origin and characteristics of the dataset employed. In addition, a short explanation on how the data are processed before being fed to the ANN, and how ANN's architecture is tuned is also provided.

2.1. Dataset

We used a dataset composed of more than 200 atactic polyacrylates and their corresponding T_g values [8,15–17] (see Table SI1). We have chosen to use the glass transition temperature as a suitable property to validate our approach due to the extensive amount of data and literature. In addition, it is a relevant property for polymers and it is related to other important properties like dynamics or viscosity among many others. For the purpose of the present work, the repeating units (monomer) of these acrylates were codified by using a Simplified Molecular Input Line Entry System (SMILES) [18,19] and converted into binary matrices (images), which are then compared to the obtained features after ANN training.

2.2. Data treatment (encoding)

As we have proposed in a recent work [14], in order to consider the structure and composition of the monomeric units, we transformed the chemical structures into linear strings by using SMILES. Then, we converted these strings into binary matrices (images) by using a one hot encoding algorithm [20] and a *dictionary* (shown below) with all the characters in the SMILES code.

Dictionary = ['c', 'n', 'o', 'C', 'N', 'O', 'F', 'P', 'S', 'Cl', 'Br', 'I', '0′, '1′, '2′, '3′, '4′, '5′, '6′, '7′, '8′, '9′, '.', '-', ' = ', '#', '$', ':', '/', '+', ')', '(', '@', '{', '}', '\', ' ', '[', ']']

It is important to note that the order of the dictionary is arbitrary and could affect the performance and the efficiency of the network. Based on our previous work [14], where all these factors were systematically analyzed, the here proposed dictionary provides both low relative errors in T_g prediction and low dispersion.

2.3. ANN's architecture

We used fully connected neural networks, fed with the previously constructed polyacrylates matrices (images) and the corresponding glass transition temperature (T_g). As mentioned, we call features to those parts of the molecule that strongly contribute to the structure-T_g relationship, being much more important for the ANN's training process than the rest of the structure. Fig. 1 shows a schematic view of the ANN's architecture: the monomer structure is codified (through SMILES) into a 2D matrix which is then flattened into a 1D vector ($X \in R^n$); this vector feeds two fully connected layers (FC_A y FC_B) with varying number of neurons, along with ReLU activations. Batch normalization [21] was employed before each activation function in order to reduce the covariance shift and to ensure a non-vanishing gradient. In addition, dropout [22] algorithm was used, with dropping probabilities ranging from 0 to 0,3. Despite error minimization, and in order to avoid any combinatory effects on the output, a dropout probability of 0 was preferred for the feature extraction process. Finally, the last hidden layer (FC_B) was connected to a single neuron (layer C) with a linear activation function responsible of providing the glass transition temperature value.

As done in our previous work [14], to ensure equal weighting of low and high T_g data values during training, the loss function was defined as the average relative error between the actual (A_i) and forecasted (F_i) glass transition temperatures.

$$Loss = \frac{100}{m_x} \cdot \sum_{i=1}^{m_x} \left(\frac{A_i - F_i}{A_i} \right)$$

An ADAM optimizer [23] with varying learning rates (lr) ranging from 0,0001 to 0,1 was employed for speeding up the convergence during training (beta 1 and beta 2 ranging from 0,1 to 0,99 and 0,1 to 0, 999, respectively). The calculations were performed by using mini batches ranging from 1 to 256 images (given the total amount of data 256 is equivalent to gradient descent).

2.4. ANN's optimization

In order to achieve the best possible performance for the ANNs before extracting features, different values of the network hyperparameters were explored. In this way, several networks with varying parameter values were trained and compared. This comparison was

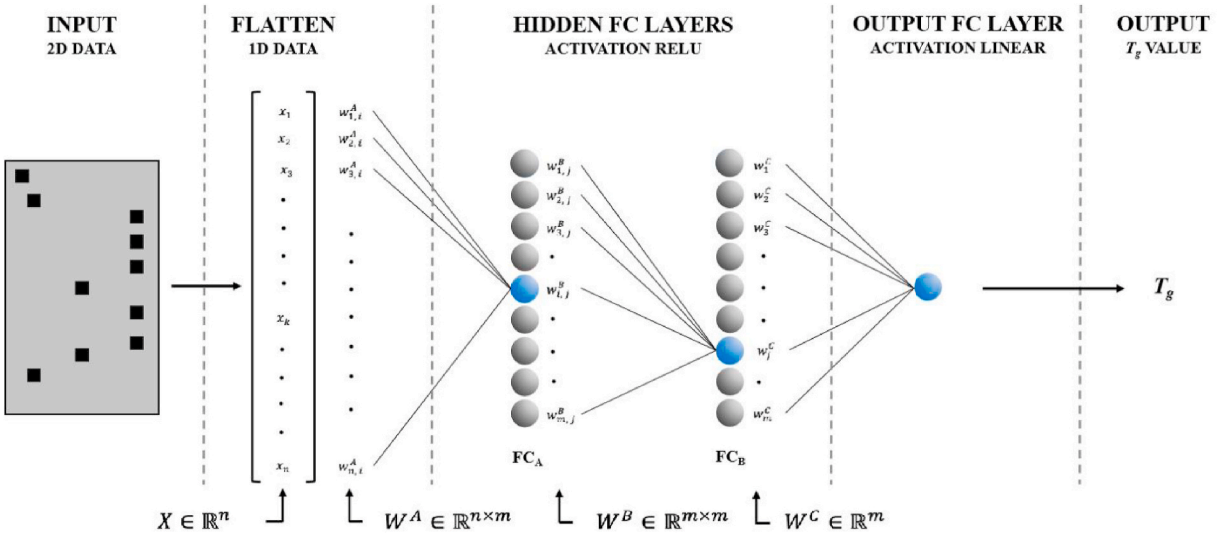

Fig. 1. Schematic picture of the artificial neural network employed for extracting the features responsible of T_g.

based on the raw performance (minimum relative error) achieved on the dataset.

As usual, the data were randomly divided into test and train subsets, and no enforcing of any preference in the way the data is divided was applied. Searching for the optimal performance of the ANNs, their hyperparameters were optimized in the following order (other important characteristics of the network were also explored, as shown in Table 1):

1. Learning rate
2. Beta 1 and beta 2
3. Mini batch size
4. # Hidden neurons in FC layers

From the above-mentioned exploration process, a confidence interval for the optimized ANN (typically larger than just the individual mean relative error) was obtained.

2.5. Features extraction

During the training process of the ANN, the input data (the codified monomer structure matrices) are flattened into a 1D vector ($X \in R^n$). This vector is then multiplied by the weights of the hidden layer A, codified in the matrix W^A ($\in R^{nxm}$). Each neuron then passes the resulting value through an activation function, which outputs a single number (per neuron), resulting in an activations vector ($\in R^m$). The whole process is repeated for these activations in the second hidden layer B, through the matrix W^B ($\in R^{mxm}$). The output of the last hidden layer is finally multiplied by the weights of the layer C ($W^C \in R^m$) and passed through a linear activation to obtain the predicted T_g value, which is then compared with the known value. From the observed difference the network then re-calculates all the weight coefficients through backpropagation [24]. The entire process is repeated several times, until the error achieves a stationary minimum value.

According to this training process, it is reasonable to think that the achieved "knowledge" of the trained ANN is largely related to the adjusted weights. Therefore, in order to know which parts of the monomers (input data) are the most relevant for determining the T_g (output data) of each polymer, we propose to "weight" the input data (monomer structure) by using the learnt coefficients (W^A, W^B and W^C). In this way, for each neuron i in layer A we can write:

$$y^A_{i,j} = x_j . w^A_{j,i} (j \in [1, n])$$

Without applying any activation function, we then pass this vector through layers B and C obtaining:

$$y^B_{i,j} = \sum_{k=1}^{m} y^A_{k,j} . w^B_{k,i} (j \in [1, n])$$

$$y^C_j = \sum_{k=1}^{m} y^B_{k,j} . w^C_k (j \in [1, n])$$

Each one of these vectors (y^A, y^B and y^C) has the same dimensions as the input data, since it is just a weighted sum of each pixel in the original data. Therefore, it is possible to reconstruct an image of these weighted inputs after each neuron in the layer, by reshaping back the vector y into its corresponding structure matrix. In particular, we will focus here on y^C at the final layer C. Thus, it can be assumed that this "weighted monomer structure", which is related to the predicted T_g value, contains the learnt knowledge about the structure-T_g relationship. A simplified scheme of this procedure is presented in Fig. SI1 (see supplementary information). In the next section we will discuss how to extract this knowledge from the weighted structure.

Table 1
Hyperparameters employed during the training of the different neural networks.

Item	Values
Data split ratio (train/test)	75/25; 80/20
Dropout probability	0; 0,2; 0,3
Mini batch size	32, 64, 128, 256
Learning rate	0,0001 to 0,01
Beta1 (Beta2)	0,1 to 0,99 (0,1 to 0,999)
# Hidden neurons	5 to 1000

3. Discussion

After determining the best set of hyperparameters for the ANN, we trained the network obtaining average relative errors for the prediction of the T_g as low as about 3% for both the training and the test sets. Some representative results of the relative error as a function of the number of epochs are presented in Fig. 2. No overfitting or relevant systematic difference between train and test errors was observed. It is worth to remind here that we are feeding the ANN only with the monomer chemical structure without any other physical or chemical input data (neither measured nor calculated) except, of course, the value of the glass transition temperature as output data.

Fig. 3 shows real vs predicted values for the train (blue dots) and test (red dots) sets obtained with our trained fully connected ANN. In comparison with other purely convolutional neural network approaches that we have used in the past [14], the number of parameters (and calculations) is larger; however, this method does not discard any information throughout calculations (in contrast with the poolings [25] and strided convolution operations that toss out parts of the input image in typical convolutional neural network approaches). Thus, the here proposed approach allows to keep unaltered the shape (or structure) of the input data (monomer structure) through all the process across the different layers.

In spite of the so obtained low errors, our aim is not only to predict the T_g but to use the implicit "knowledge" of the trained network to get some insight about the portions of the molecular structure that are more directly involved in determining the value of the glass transition temperature.

Once the ANN is trained to minimize the relative error for predicting

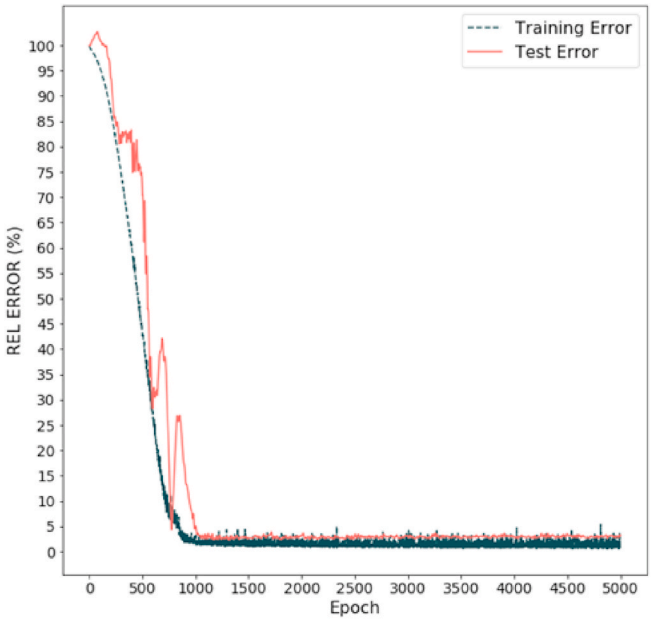

Fig. 2. Average relative error for the prediction of the glass transition temperature as a function of the epoch number.

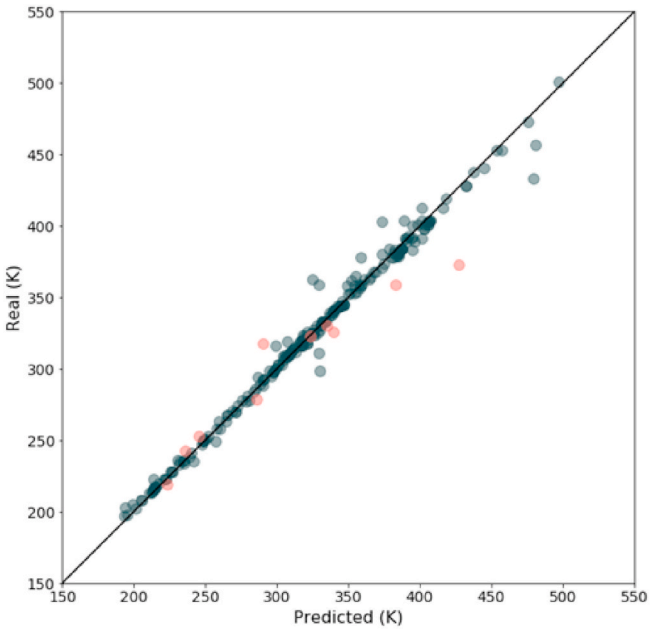

Fig. 3. Real vs predicted T_g values obtained from the trained ANN. Blue and red dots stand for train and control values, respectively. (For interpretation of the references to color in this figure legend, the reader is referred to the Web version of this article.)

the T_g, the feature extraction method described in the previous section allows to "see" how the network weights each part of the monomer structure. The matrix y^C at the output of the ANN represents the monomer structure weighted by the implicit "knowledge" learnt by the trained network.

Fig. 4 shows input images for selected control monomers (as obtained after the SMILE encoding); by definition, all the points (matrix elements) are one (full red according to the color bar scale). After multiplying this matrix by the corresponding weights (W^A, W^B and W^C) we obtain the output structure as shown on the right column in Fig. 4. In this case, each dot (matrix element) has a continuous value represented in Fig. 4 by a certain color: redder for those parts of the monomer that are more relevant for increasing the T_g, and bluer when the effect is the opposite. In order to facilitate the interpretation of the data, the chemical structure of the monomers is also shown (see insets in Fig. 4). On the right column a color map has been overlapped to the chemical structure to highlight the role of the different parts of the monomer on the T_g value. The color map is created from the output "weighted" structure, considering that each element in the structure matrix represents a part of the monomer and the corresponding value is codified into a color scale. Other monomers from the control group are shown in Fig. SI2 (see supplementary information).

For the employed acrylates dataset, three general trends that closely follow polymer science reported behaviors [26–30] can be observed:

a) The presence of certain species adjacent to the monomer's functional group is positively weighted (e.g. as shown in Fig. 4a and b the presence of a methyl group in methacrylates increases T_g). This behavior has been largely reported, and it is related to the change in the backbone stiffness of the polymer [26,31–33]. In this sense, the ANN is able to capture this effect, which can cause T_g differences of about 100 K between PMMA and PMA. Chain stiffness is known to play a major role in determining the T_g of a polymer: Flory [31] has described this chain stiffening by energy parameter ε which appears when two consecutive bonds along a chain are not collinear (while no energy is present if they are).

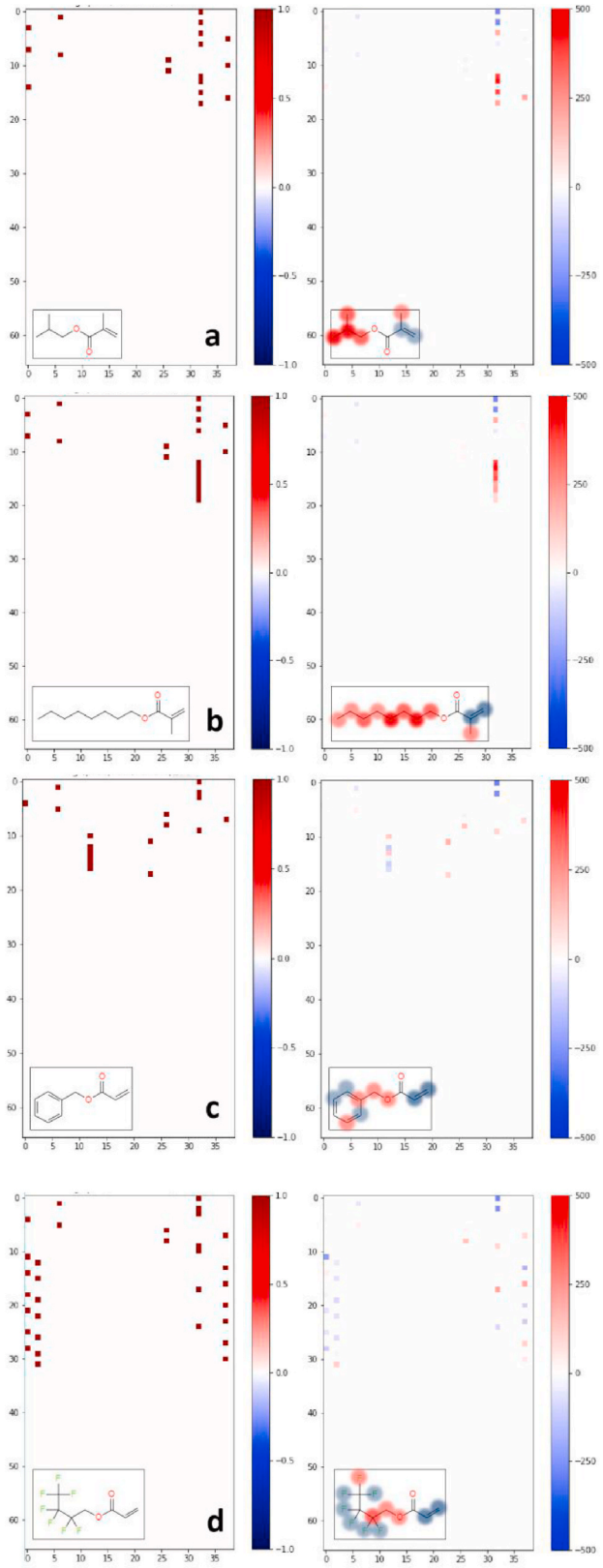

Fig. 4. Input data and chemical structure (left), and degree of activation produced by the ANN (right), for selected control monomers: a) Poly(isobutyl methacrylate), b) Poly(octyl methacrylate), c) Poly(benzyl acrylate) and d) Poly (1H,1H-heptafluorobutyl acrylate). Axes represent the position of each character in the dictionary (x axes) and the position of each character on the corresponding SMILES code for the given polymer (y axes).

Therefore, the presence/absence of adjacent species heavily modifies this parameter and in turn the observed chain stiffness. The chain stiffness, however, it's not the only property affecting glass transition; even polymers with no chain stiffness present glass transition temperatures (e.g. polydimethylsiloxane [34]). In addition, chain stiffness it's not relevant for very low molecular weight organic glasses (which in turn generally behave as polymeric glasses). Finally, it is important to note that the effect of the main polymer chain is diluted as the monomer tail becomes larger (an effect also detected by our ANN, as shown in Fig. 4b).

b) Size, shape and stiffness of the side groups (or "tail"). Generally speaking, with everything else kept constant, the bigger the volume occupied by a rigid tail, the larger the observed glass transition temperature. As an example, the presence of a *t*-butyl group in p-position tends to increase the detected T_g, while a *N*-butyl group tends to decrease it. In the same way, the presence of alkyl chains can also cause changes [35–37] (the longer the alkyl chain the lower the observed glass transition temperature). Fig. 4a–c also show that the effect of the presence/absence and composition of this side chain is detected by the ANN. Thinking the energy barrier to chain movements as composed by two contributions [35]: 1) actual rotation energy around bonds and 2) resistance of the surrounding medium, it is noteworthy that a linear tail decreases the last one. Furthermore, this "lubricating" effect produced by the linear chain can be also analyzed in terms of length and substitutions: hydrocarbonated chains produce a different (quantitatively) lubricating effect than a fluorinated one [34,38–40]. As a result, fluorinated chains are weighted differently during training (as shown in the heatmap of Fig. 4d), and T_gs are larger. As expected, the same kind of effect is observed when the bulkier phenyl groups are incorporated, as shown in Fig. 4c.
c) The combination of any of the formers defines several T_g groups: 1) a very large predicted T_g value when phenyl groups are introduced in the monomer's tail and methyl groups are present as adjacent species; 2) a very small predicted T_g value when fluorinated linear chains are present in the monomer's tail and no adjacent species are introduced; and 3) intermediate combinations.

Fig. 5 shows the control group monomers structures and an overimposed ANN's "attention" heat map. In addition to the structures, real and predicted glass transition temperatures are presented next to each monomer (in black and grey, respectively). Generally speaking, we could divide the control group into three main branches starting from poly(methylmethacrylate): a) increasing the number of atoms in the pending chain [A1 poly(ethyl methacrylate) and B1 poly(octyl methacrylate)]; b) other geometries in the pending chain [D1 poly(isobutyl methacrylate) and D2 poly(terbutyl methacrylate)]; and c) substitution of methyl by other species (C1), no methyl (C2), introduction of phenyl groups (C3 and C4) and fluorination (E1).

The results point to the previously mentioned sub structures within the monomers, which in turn show that the ANN tends to identify chemically meaningful features responsible for determining the T_g value. Thus, linear side chains are strongly weighted, as illustrated by the heatmaps that go through A1-B1-C1-E1, along with their "lubricating" effect and composition. Geometry is also highlighted, as shown though D1 and D2. Regarding this effect, it is also noteworthy the effect of bulkier phenyl groups (as shown in C3), the addition of a single atom to the side chain effect (C4), and how in all cases the ANN focus the attention in these features.

It is worth mentioning here that we didn't make any assumption about the role of free volume and the inter-chain interaction on the glass transition temperature. In principle, any inter-molecular contribution is implicitly related to the chemical structure of the monomer and therefore it should be "seen" by the ANN. Moreover, we can use this approach, in combination with experiments where the pressure-temperature dependence of the T_g is measured, to quantify and decouple the contributions from intra- (intrinsic rotational barriers) and inter-molecular (free volume/local packing) interactions [41]. Some work in this sense is currently being done and will be published soon.

In summary, from the chemical point of view many different factors have been reported to affect the T_g values of polymers, being intermolecular forces, chain stiffness and geometry the most important ones. The presence of bulky groups (as phenyl rings) can be diluted by long alkyl chains, while the lubricating effect of long alkyl chains can be hidden by very stiff backbones. The ANN based approach proposed in this work has shown to be able to recognize these features and to quantify its relevance in the glass transition temperature value. It is important to highlight here that this knowledge is self-learnt by the network based only on the monomer chemical structure and the corresponding T_g value. This approach could substantially help to gain both qualitative and quantitative insights of the behavior of the polymeric materials, especially for those properties which are difficult and/or expensive to measure. It is also expected that unknown features can be unveiled by this approach.

4. Conclusions

The feasibility of using a fully connected neural network architecture for extracting features related to the glass transition temperature of

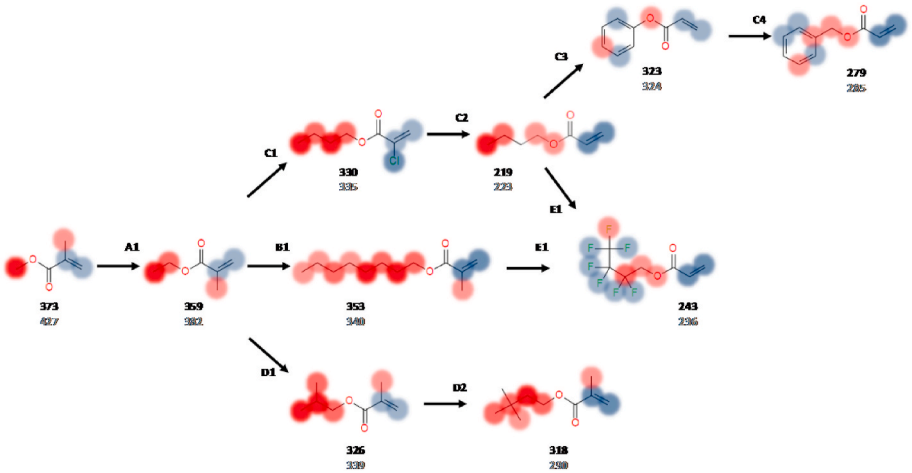

Fig. 5. Control group monomer structures with their corresponding attention heatmap as obtained from the trained ANN (the real (black) and predicted (grey) T_g values are indicated next to each monomer).

polymers has been demonstrated. We have shown that the implicit knowledge acquired by the ANN while trained to predict the T_g value, can be used to localize and quantify the intra-monomer contributions to the glass transition temperature. This approach relies only on the knowledge of the repeating unit chemical formula and does not require any kind of experimental measurements or calculations as input, therefore becoming a powerful designing tool for material scientists and engineers.

Declaration of competing interest

The authors declare that they have no known competing financial interests or personal relationships that could have appeared to influence the work reported in this paper.

CRediT authorship contribution statement

Luis A. Miccio: Conceptualization, Methodology, Software, Validation, Formal analysis, Investigation, Data curation, Writing - original draft, Writing - review & editing, Visualization, Supervision, Supervision, Project administration, Funding acquisition. **Gustavo A. Schwartz:** Conceptualization, Methodology, Software, Validation, Formal analysis, Investigation, Data curation, Writing - original draft, Writing - review & editing, Visualization, Supervision, Supervision, Project administration, Funding acquisition.

Acknowledgment

We gratefully acknowledge the financial support from the Spanish Government “Ministerio de Ciencia e Innovación” (PID2019-104650GB-C21) and the Basque Government (IT-1175-19). We also acknowledge the support of NVIDIA Corporation with the donation of the Titan V GPU used for this research.

Appendix A. Supplementary data

Supplementary data to this article can be found online at https://doi.org/10.1016/j.polymer.2020.122786.

References

[1] A.-L. Barabási, H.G. Schuster, Applied Statistics for Network Biology Methods in Systems Biology Statistical Modelling of Molecular Descriptors in QSAR/QSPR Statistical Diagnostics for Cancer Analyzing High-Dimensional Data Reviews of Nonlinear Dynamics and Complexity, vol. 1, 2010, 978–3.
[2] S.J. Joyce, D.J. Osguthorpe, J.A. Padgettf, G.J. Price, Y. Ba, Neural Network Prediction of Glass-transition Temperatures from Monomer Structure, vol. 91, 1995, pp. 2491–2496.
[3] S.B. Lo, et al., Artificial convolution neural network techniques and applications for lung nodule detection, IEEE Trans. Med. Imag. 14 (1995) 711–718.
[4] C.W. Ulmer, D.A. Smith, B.G. Sumpter, D.I. Noid, Computational neural networks and the rational design of polymeric materials: The next generation polycarbonates, Comput. Theor. Polym. Sci. 8 (1998) 311–321.
[5] G.A. Schwartz, Prediction of rheometric properties of compounds by using artificial neural networks, Rubber Chem. Technol. 74 (2001) 116–123.
[6] B.E. Mattioni, P.C. Jurs, Prediction of glass transition temperatures from monomer and repeat unit structure using computational neural networks, J. Chem. Inf. Comput. Sci. 42 (2002) 232–240.
[7] Z. Zhang, K. Friedrich, Artificial neural networks applied to polymer composites: A review, Compos. Sci. Technol. 63 (2003) 2029–2044.
[8] C. Bertinetto, et al., Prediction of the Glass Transition Temperature of (Meth) Acrylic Polymers Containing Phenyl Groups by Recursive Neural Network, vol. 48, 2007, pp. 7121–7129.
[9] W. Liu, C. Cao, Artificial Neural Network Prediction of Glass Transition Temperature of Polymers, 2009, pp. 811–818, https://doi.org/10.1007/s00396-009-2035-y.
[10] Y. Liu, T. Zhao, W. Ju, S. Shi, Materials discovery and design using machine learning, J. Mater. 3 (2017) 159–177.
[11] F. Hou, et al., Comparison study on the prediction of multiple molecular properties by various neural networks, J. Phys. Chem. 122 (2018) 9128–9134.
[12] Z. Jiang, Z. Zhang, K. Friedrich, Prediction on wear properties of polymer composites with artificial neural networks, Compos. Sci. Technol. 67 (2007) 168–176.
[13] X. Zheng, P. Zheng, L. Zheng, Y. Zhang, R. Zhang, Multi-channel convolutional neural networks for materials properties prediction, Comput. Mater. Sci. 173 (2020) 109436.
[14] L.A. Miccio, G.A. Schwartz, From chemical structure to quantitative polymer properties prediction through convolutional neural networks, Polymer 193 (2020) 122341.
[15] D.J. Plazek, K.L. Ngai, The glass temperature, in: J.E. Mark (Ed.), Physical Properties of Polymers Handbook, vol. 187–215, Springer, New York, 2007.
[16] Plastic Library, Chemical Retrieval on the Web, CROW. Chemical Retrieval on the Web, CROW, 2019. https://polymerdatabase.com.
[17] G. Wypych, Handbook of Polymers, Elsevier, 2016.
[18] D. Smiles Weininger, A chemical language and information system. 1. Introduction to methodology and encoding rules, J. Chem. Inf. Comput. Sci. 28 (1988) 31–36.
[19] N.M. O'Boyle, Towards a Universal SMILES representation - a standard method to generate canonical SMILES based on the InChI, J. Cheminform. 4 (2012) 22.
[20] H. Alkharusi, Categorical variables in regression analysis: A comparison of dummy and effect coding, Int. J. Educ. 4 (2012) 202–210.
[21] S. Ioffe, C. Szegedy, Batch Normalization: Accelerating Deep Network Training by Reducing Internal Covariate Shift, 2015 arXiv1502.03167 [cs].
[22] N. Srivastava, G. Hinton, A. Krizhevsky, I. Sutskever, R. Salakhutdinov, Dropout: A simple way to prevent neural networks from overfitting, J. Mach. Learn. Res. 15 (2014) 1929–1958.
[23] D.P. Kingma, J. Adam Ba, A Method for Stochastic Optimization, 2014 arXiv1412.6980 [cs].
[24] D.E. Rumelhart, G.E. Hinton, R.J. Williams, Learning representations by back-propagating errors, Nature 323 (1986) 533–536.
[25] H. Wu, X. Gu, Max-pooling Dropout for Regularization of Convolutional Neural Networks, 2015 arXiv1512.01400 [cs].
[26] J.H. Gibbs, E.A. DiMarzio, Nature of the glass transition and the glassy state, J. Chem. Phys. 28 (1958) 373–383.
[27] R.H. Boyd, Relaxation processes in crystalline polymers: Molecular interpretation - A review, Polymer (Guildf). 26 (1985) 1123–1133.
[28] F. Kremer, A. Schönhals, Broadband Dielectric Spectroscopy, 2003.
[29] L.A. Miccio, J. Otegui, M.E. Penoff, P.E. Montemartini, G.A. Schwartz, Fluorinated networks dynamics studied by means of broadband dielectric spectroscopy, J. Appl. Polym. Sci. 132 (2015).
[30] M.M. Kummali, A. Alegría, L.A. Miccio, J. Colmenero, Study of the dynamic heterogeneity in poly(ethylene-ran-vinyl acetate) copolymer by using broadband dielectric spectroscopy and electrostatic force microscopy, Macromolecules 46 (2013).
[31] T.G. Fox, P.J. Flory, Second-order transition temperatures and related properties of polystyrene. I. Influence of molecular weight, J. Appl. Phys. 21 (1950) 581–591.
[32] J.H. Gibbs, Nature of the glass transition in polymers, J. Chem. Phys. (1956) 25 185–186.
[33] Statistical thermodynamics of semi-flexible chain molecules, Proc. R. Soc. London. Ser. A Math. Phys. Sci. 234 (1956) 60–73.
[34] R.F. Boyer, The relation of transition temperatures to chemical structure in high polymers, Rubber Chem. Technol. (1963) 36 1303–1421.
[35] C.G. Overberger, L.H. Arond, R.H. Wiley, R.R. Garrett, Monomers containing large alkyl groups. IV. Polymerization and properties of the polymers of 2-alkyl-1,3-butadienes, J. Polym. Sci. 7 (1951) 431–441.
[36] E.F. Jordan, D.W. Feldeisen, A.N. Wrigley, Side-chain crystallinity. I. Heats of fusion and melting transitions on selected homopolymers having long side chains, J. Polym. Sci. Part A-1 Polym. Chem. 9 (1971) 1835–1851.
[37] M.L. Dannis, Thermal expansion measurements and transition temperatures, first and second order, Rubber Chem. Technol. 32 (1959) 1005–1015.
[38] F.A. Bovey, J.F. Abere, G.B. Rathmann, C.L. Sandberg, Fluorine-containing polymers. III. Polymers and copolymers of 1,1-dihydroperfluoroalkyl acrylates, J. Polym. Sci. 15 (1955) 520–536.
[39] L.A. Miccio, D.P. Fasce, W.H. Schreiner, P.E. Montemartini, P.A. Oyanguren, Influence of fluorinated acids bonding on surface properties of crosslinked epoxy-based polymers, Eur. Polym. J. 46 (2010).
[40] L.A. Miccio, R. Liaño, P.E. Montemartini, P.A. Oyanguren, Partially fluorinated polymer networks: Synthesis and structural characterization, J. Appl. Polym. Sci. 122 (2011).
[41] G. Floudas, K. Mpoukouvalas, P. Papadopoulos, The role of temperature and density on the glass-transition dynamics of glass formers, J. Chem. Phys. 124 (2006), 074905.